Divergent roles for KLF4 and TFCP2L1 in Naive Ground State Pluripotency and Human Primordial Germ Cell Development

Grace V Hancock
Molecular Biology Institute, University of California Los Angeles
Wanlu Liu
Zhejiang University-University of Edinburgh Institute
Lior Peretz
Department of Molecular Cell and Developmental Biology, University of California, Los Angeles
Di Chen
Department of Molecular Cell and Developmental Biology, University of California, Los Angeles
Joanna J Gell
Department of Pediatrics, David Geffen School of Medicine
Amanda J Collier
Department of Biological Chemistry, David Geffen School of Medicine
Jesse R Zamudio
Department of Molecular Cell and Developmental Biology, University of California, Los Angeles
Kathrin Plath
Department of Biological Chemistry, David Geffen School of Medicine
Amander T Clark (clarka@ucla.edu)
Department of Molecular Cell and Developmental Biology, University of California, Los Angeles

Research Article

Keywords: Pluripotency, Primordial Germ Cells, PGCs, KLF, TFCP2L1, Naive, Stem Cells, hESCs, Human

Posted Date: April 24th, 2020

DOI: https://doi.org/10.21203/rs.3.rs-24873/v1

Version of Record: A version of this preprint was published at Stem Cell Research on August 1st, 2021.
See the published version at https://doi.org/10.1016/j.scr.2021.102493.

Abstract

During development, human primordial germ cells (hPGCs) transition through a transcriptional and epigenetic state similar to pre-implantation naive ground state epiblast cells. In hPGCs, this state is called naive-like ground state pluripotency. Diagnostic transcription factors that define this state include TFAP2C, KLF4, and TFCP2L1, with TFAP2C necessary for both establishment of the naive-like ground state in hPGC-like cells (hPGCLCs) and establishment of naive ground state human embryonic stem cells (hESCs). Here, we show that KLF4 and TFCP2L1 are not required for hPGC specification or establishment of the naive-like ground state in hPGCLCs. Instead, KLF4 and TFCP2L1 are each required for reversion of primed hESCs to the self-renewing naive ground state. Additionally, TFCP2L1 but not KLF4 function after hPGC specification in the proliferation and survival of hPGCLCs.

Introduction

Human peri-implantation development involves a series of developmental transitions through a spectrum of pluripotent states. These include the conversion of NANOG positive inner cell mass (ICM) cells in the naive ground state to pre-implantation and early post implantation pluripotent epiblast cells, followed by a final pluripotent transition to post-implantation primed epiblast cells. These primed cells differentiate and ultimately disappear following gastrulation[1–3]. The “naive ground state”, defined as the globally demethylated pre-implantation epiblast cells, has been recapitulated as a distinct self-renewing state *in vitro* from human embryonic stem cells (hESCs) and human induced pluripotent stem cells (hiPSCs) [4–6]. A naive-like ground state has also been reported in human primordial germ cells (hPGCs) *in vivo* and hPGC-like cells (hPGCLCs) *in vitro*[7,8]. Naive ground state pluripotent stem cells and naive-like ground state hPGCs/hPGCLCs have definable common characteristics, including genome-wide DNA demethylation and a transcriptome that is more closely related to each other than to primed hESCs/hiPSCs. Furthermore, female naive ground state hESCs, hiPSCs and hPGCs are reported to have two active X chromosomes [6,9,10]. Despite these similarities, hPGCs and pluripotent cells of the peri-implantation embryo *in vivo* also have unique molecular features, notably the expression of NANOS3 in hPGCs, and Krupple like family 17 (KLF17) in the naive ground state, which in addition to their clear stage-specific differences, serve to define these cell types as distinct [11,12].

Human PGCs are specified from a peri-implantation pluripotent progenitor around the time of embryo implantation. Although the exact nature of this progenitor has not been fully characterized, it appears that hPGCs are specified during the peri-implantation pluripotent cell transition through a TFAP2A positive state, and could arise from amnion and/or gastrulation-like cells [13–15]. Once specified, hPGCs exhibit a naive-like ground state pluripotent identity, but are not functionally pluripotent, as the fate of hPGCs is to differentiate only into gametes. Dis-regulation of this fate can lead to germ cell tumors, or loss of the germline[16,17]. Understanding this acquisition or potential maintenance of naive-like ground state pluripotency in hPGCs may provide critical insights into the similarities and differences between functional pluripotency in cells of the peri-implantation embryo and the unipotency of hPGCs.

In humans, the transcription factor TFAP2C is required for both naive ground state pluripotency and the specification of hPGCLCs from hESCs [7,18,19]. In hPGC development, TFAP2C functions to prevent expression of somatic gene expression programs, and also to turn on the transcriptional program of naive-like ground state pluripotency[13,19]. This leads to the question of whether other naive ground state pluripotent transcription factors are also required for hPGCLC specification. Two critical transcription factors required for naive ground state pluripotency *in vitro*, that are also expressed in pre-implantation human embryos *in vivo* are Transcription Factor CP2-like protein 1 (TFCP2L1) and KLF4 [5]. TFCP2L1 was initially discovered in mouse ESCs (mESCs) as a target of the LIF / STAT3 pathway where it is functionally required to revert primed mESCs to the naive state [20]. The KLF binding motif is highly enriched in primate-specific enhancers located in differentially open chromatin in pre-implantation embryos. In an *in vitro* assay with primed human pluripotent stem cells, these enhancers were activated when either KLF4 or KLF17 were over-expressed and bound to the KLF motif[21]. KLF17 in not transcriptionally expressed in hPGCs, whereas *KLF4* and *TFCP2L1* are highly up-regulated in naive ground state hESCs and hPGCs[5,8,11–13], and both KLF4 and TFCP21 are independently required for self-renewal in the human naive ground state media called titrated two inhibitor, LIF, Go6983 (t2iLGo) [5]. Although, these transcription factors are required for maintaining self-renewal of human naive ground state pluripotent stem cells, their role in specification of hPGCLCs is unknown.

In the current study, we evaluated the protein expression of KLF4 and TFCP2L1 in hPGCs *in vivo* and with hPGCLC differentiation *in vitro*. In addition, we evaluated the functional role of KLF4 and TFCP2L1 in establishing naive-like ground state in hPGCLCs *in vitro* using CRISPR/Cas9.

Results

TFCP2L1 and KLF4 expression in hPGC development

To further characterize KLF4 and TFCP2L1 in hPGC development, we used the *in vitro* model of hPGC specification by differentiating hPGCLCs from hESCs. To determine if *KLF4* and *TFCP2L1* are uniquely upregulated in hPGCLCs in this differentiation model, we used fluorescence activated cell sorting (FACS) with conjugated antibodies that recognize Integrin alpha-6 (ITGA6) and epithelial cell adhesion molecule (EPCAM) to separate the hPGCLC population at day 4 (D4) of aggregate differentiation[22,23] and performed semi quantitative reverse transcriptase polymerase chain reaction (RT-PCR). Our results show that the hPGC markers *PRDM1, SOX17* and *TFAP2C* are significantly up regulated in hPGCLCs relative to undifferentiated hESCs, incipient mesoderm-like cells (iMeLCs) and somatic cells indicating the specificity of the FACS strategy to isolate hPGCLCs. Similarly, we also identified *KLF4* and *TFCP2L1* as being significantly upregulated in the hPGCLCs at D4 relative to undifferentiated hESCs(Fig. 1a).

Next, we performed immunofluorescence of aggregates at D4 to evaluate KLF4 and TFCP2L1 protein expression. We discovered that KLF4 was co-expressed with TFAP2C/PRDM1 double positive hPGCLCs, while TFCP2L1 protein was not detected at all indicating post-transcriptional regulation of TFCP2L1 in hPGCLCs (Fig. 1b). To verify this result, we evaluated hPGCLC specification at D4 using two additional

hESC lines, UCLA1 (46, XX) and UCLA2 (46, XY) (Supplementary Figure 1a,b), which were also negative. This result indicates that repression of TFCP2L1 protein at D4 is common to the differentiation of hPGCLCs across multiple independently derived hESC lines.

To evaluate protein expression beyond hPGC specification, we next evaluated KLF4 and TFCP2L1 protein using embryonic and fetal gonadal samples consented to research from D74 to D140 post fertilization. Here, we discovered that KLF4 and TFCP2L1 protein are expressed in the cKIT+ hPGCs at all stages of male and female hPGC development (Fig. 1c). In addition, we discovered that KLF4 protein was also expressed in some rare somatic cells within the fetal testis and ovary, while TFCP2L1 protein was specific to the cKIT+ hPGCs (Fig. 1c). The tyrosine kinase receptor cKIT is a diagnostic marker of hPGCs in the embryonic and fetal human gonad, and is expressed on the surface of the hPGCs[12]. In contrast the KLF4 and TFCP2L1 transcription factors are localized to the nucleus (Fig. 1c). However, we noted that there were sex differences between male and female cKIT+ hPGCs, with a lower percentage of cKIT+ female hPGCs expressing KLF4 and TFCP2L1 in general, compared to cKIT+ male hPGCs. This was particularly noteworthy at the later developmental time points and is most likely due to the differentiation of the female cKIT+ hPGCs into oocytes (Fig. 1d, and Supplementary Figure 1c), which is a stage when the pluripotency-like program is repressed as the meiotic program is initiated[24]. Taken together the dynamic regulation of TFCP2L1 and KLF4 protein in hPGCLCs may suggest that KLF4 functions independently during hPGC specification, whereas the co-expression of TFCP2L1 and KLF4 in hPGCs may suggest that these transcription factors function coordinately at a later stage.

KLF4 is not required for hPGC specification

Given that KLF4 protein is expressed in hPGCLCs, we next used CRISPR-Cas9 gene editing to evaluate whether KLF4 has a role in hPGCLC specification. We produced two KLF4-null mutant hESC subclones in the UCLA1 hESC line (#35 and #43) and selected a wild type subclone as a control. Confirmation of the mutation was achieved by genotyping and Sanger sequencing of the mutant clones (Supplementary Figure 2b). Immunofluorescence for KLF4 protein at D4 of differentiation revealed that the CRISPR alleles created null mutations with no detectable KLF4 protein in either mutant subclone (Fig. 2a). Despite the loss of KLF4, our results show that the hPGCLC markers (TFAP2C and PRDM1) are still co-expressed in the KLF4 null mutant mutant sublines (Fig. 2a). To evaluate hPGCLC specification using an alternate approach, we quantified the percentage of hPGCLC by FACS at D4 using the hPGCLC surface marker combination of ITGA6 and EPCAM (Fig. 2b), quantified in (Fig. 2c). This result yielded no statistically significant difference in the percentage of specified hPGCLCs between KLF4 mutants and controls at D4.

Given that KLF4 is a transcription factor, we next we sought to evaluate whether the KLF4 null mutant hPGCLCs at D4 had an altered transcriptome despite evidence of a PRDM1/TFAP2C hPGC identity. To achieve this, we created a third mutant and control CRISPR/Cas9 null mutant subline in the H1 OCT4-GFP (46, XY) hESC line, isolated the hPGCLCs by FACS using ITGA6 and EPCAM, and performed RNA sequencing (RNA-Seq) at D4 in biological duplicate. This result revealed that the KLF4 null mutant and control transcriptomes were largely the same (Fig. 2d), with only a small number of differentially

expressed genes (DEGs) between mutant and control hPGCLCs. In comparing normalized read counts, KLF4 was significantly down regulated in the mutant hPGCLCs (Supplementary Figure 2a), and the other DEGs including Aconitase1 (ACO1), Carboxylesterase 1 (CES1), Succinate-CoA GDP-Forming Beta Subunit (SUCLG2) and Zinc Finger Protein 254 (ZNF254) are not known to have a role in pluripotency or hPGC development. Additionally, in evaluating specific genes of interest related to naive and primed pluripotency and hPGC development, we discovered equivalent expression of these diagnostic genes between control and mutant hPGCLCs (Fig. 2e). Taken together, these results indicate that while KLF4 is highly upregulated upon hPGC specification, it is not functionally required for the specification of hPGCLCs at D4, and is not a master regulator of hPGC transcription.

KLF4 and TFCP2L1 are required for re-establishment of the naive ground state

Given that KLF4 is expressed but not required for hPGC specification, we next turned to the primed-naive reversion model to evaluate whether KLF4 is required for establishment of the naive ground state. Previous studies have shown that KLF4 and TFCP2L1 are each required for self-renewal under the naive ground state condition called t2iLGo[5]. However, it is not known whether KLF4 or TFCP2L1 are required for reversion from the primed to the naive ground state, a phenomenon that occurs as hPGCLCs differentiate from primed hESCs.

To evaluate this, we developed a CRISPR/Cas9 deletion line of TFCP2L1 in the primed state, and evaluated KLF4 and TFCP2L1 mutant and control lines in reversion of primed hESCs to the naive ground state using the media called 5 inhibitor LIF, FGF2/ ACTIVIN (5iLF/A) published previously [6,18]. Mutations at the TFCP2L1 locus were confirmed by Sanger sequencing (Supplemental Figure 2b). Upon induction of naive-ground state conditions, we discovered that the morphology between the KLF4 and TFCP2L1 mutant and control lines were noticeably different by D10 of reversion in 5iLF/A, with typical dome-shaped colonies emerging by passage 3 (P3) in the controls, but not in the KLF4 or TFCP2L1 mutants (Fig. 3 a,c). To quantify this, we scored colonies by their morphological appearance at each passage, as either differentiated/primed or primed/naive (transition) or naive (Fig. 3b,d). This result revealed that by P3 the mutant lines were composed of very few colonies relative to controls at P1, and what remained was either in the differentiated/primed category or composed of a transitional primed/naive colonies.

To quantify this using an alternate approach, we performed immunofluorescence for the naive ground state marker KLF17[11] at P3. This result shows that control reversions exhibited discreet naive colonies with co-expression of OCT4 and KLF17, whereas in the KLF4 and TFCP2L1 mutant lines, KLF17 was scattered and heterogeneously expressed. When KLF17 was expressed it was localized to loosely packed OCT4+ cells consistent with a transitional naive/primed state (Fig. 3e-h).

Using a third approach, we used flow cytometry at P3, corresponding to D18 of reversion to quantify the percentage of naive ground state cells [26]. We chose CD75 as the most stringent cell-surface marker for naive ground state cell identity, and CD24 as a surface marker to identify primed cells. Human cells were first selected by excluding CD90.2-expressing mouse cells. Consistent with immunofluorescence and

morphology, we discovered that in control reversions at P3, 25-50% of human cells were CD75 positive consistent with a naive ground state identity, whereas the KLF4 and TFCP2L1 mutant sublines had 3-fold and 10-fold fewer naive ground state cells respectively (Fig. 3 i,j). Furthermore, in the mutant cell lines, CD24 expression was detectable, indicating an inability to repress the primed identity. Thus, KLF4 and TFCP2L1 function in the establishment of naive ground state pluripotency in pluripotent stem cells, but KLF4 does not have a role in the establishment of naive-like ground state pluripotency in hPGCLCs.

TFCP2L1, but not KLF4 contribute to early hPGC development

Since critical aspects of naive-like ground state pluripotency such as genome-wide DNA demethylation do not occur until D20 in early nonhuman primate PGCs[15]. Therefore, we next evaluated a potential role for KLF4 and TFCP2L1 with extended culture of hPGCLCs to D25, when hPGCLCs initiate DNA demethylation[27] (Fig. 4a and Supplementary Fig. 3a). To achieve this, we used FACS to isolate D4 hPGCLCs with ITGA6/EPCAM, and cultured the hPGCLCs for an additional 10 and 21 days, corresponding to D14 and D25 after hPGCLC specification[27].

Using FACS to isolate control and TFCP2L1 mutant hPGCLCs at D4, revealed that as expected, that TFCP2L1 had no role in hPGCLC specification as determined by ITGA6/EPCAM staining (Fig. 4b). During the course of extended culture, we discovered that in wild type and control hPGCLCs, TFCP2L1 protein becomes detectable in the PRDM1/TFAP2C double positive hPGCLCs by D10 (Supplemental Figure 4b), and TFCP2L1 protein expression is maintained in the hPGCLCs until at least D4C21 (Fig. 4c). This result indicates that TFCP2L1 protein is dynamically regulated during hPGCLC development *in vitro* becoming stably expressed after hPGCLC specification

In order to evaluate the role of TFCP2L1 in hPGCLC development, we generated extended cultures of TFCP2L1 mutant and control sublines, and evaluated germ cell identity by co-immunofluorescence for PRDM1/TFAP2C (Fig. 4d). This result shows that in the absence of TFCL2L1 protein, PRDM1/TFAP2C hPGC identity is maintained similar to control. However, at D4C21, we noticed that the number of colonies and the number of cells within a colony was reduced in the TFCP2L1 mutant hPGCLCs relative to controls (Fig. 4 d,e). In order to evaluate whether proliferation was affected, we performed Edu staining at D4C21 and show that the fraction of Edu+ hPGCLCs is significantly less than controls (Fig. 4 f,g).

Given the role for TFCP2L1 in hPGCLC proliferation and survival, we repeated these experiments using the KLF4 mutant and control lines, and unlike TFCP2L1, we found no difference at any time point in the KLF4 mutants relative to the control (Supplementary Figure 4a-e).

Discussion

Our results highlight notable differences between the mechanisms responsible for establishing the naive ground state of pluripotency in human pre-implantation embryos/human pluripotent stem cells, and the naive-like ground state pluripotency of hPGCs/hPGCLCs. In previous studies, it was shown that the naive transcription factor TFAP2C binds to and opens naive enhancers to regulate the establishment and

maintenance of naive ground state pluripotency from primed human pluripotent stem cells, as well as the specification and reacquisition of naive-like ground state pluripotency in hPGCLCs [7,18]. In the current study, we evaluated two additional master regulators of naive ground state pluripotency, KLF4 and TFCP2L1, which in previous studies were reported to regulate self-renewal of naive ground state pluripotent stem cells in t2iLGo [5], and KLF4 was required to open naive enhancers similar to TFAP2C[21]. However, our data showed that KLF4 and TFCP2L1 are not required for hPGCLC specification and re-acquisition of naive-like ground state pluripotency that begins in hPGCLCs at D4. Instead, KLF4 and TFCP2L1 were each required for establishing naive ground state of pluripotency as represented by reverting primed pluripotent stem cells to the naive state *in vitro*. Therefore, although a common transcriptional program can be identified in naive-ground state pluripotency and hPGCs, only TFAP2C has a role in establishing the naive-like ground state of pluripotency in hPGCs, whereas KLF4 and TFCP2L1 do not.

Mechanistically, TFCP2L1 has been shown to target the KLF4 promoter, and to also bind KLF4 protein, highlighting that these transcription factors function in combinatorial roles to regulate the self-renewing naive ground state in humans [28]. The KLF family binding motif is enriched in pre-implantation naive enhancers called TEENhancers, and these are activated by both KLF4 and KLF17 and can recruit OCT4[21]. Although we observed KLF4 protein at the time of hPGCLC specification, TFCP2L1 protein was not expressed until hPGCLCs were cultured in extended culture and KLF17 is not expressed by hPGCs/hPGCLCs at any stage[7,8,10,12]. This uncoupling of TFCP2L1 and KLF17 protein expression from KLF4 at the time of hPGCLC specification may be necessary to avoid re-establishment of functional naive-ground state pluripotency, and therefore a protective mechanism to reduce the risk of embryonal carcinoma type germ cell tumor formation at the time of hPGC specification. Indeed the TFCP2L1 locus is in a haplotype block associated with testicular germ cell tumors [29].

Our results show that upon extended culture, TFCP2L1 protein becomes detectable in hPGCLCs, and that TFCP2L1 but not KLF4 regulates proliferation and survival of the hPGCLC population. Success of the hPGCLC extended culture system depends on addition of cAMP agonists including Forskolin and Rolipram[27], which increase the intracellular content of cAMP. This is important because in placental cell lines, the expression of TFCP2L1 protein is associated with cAMP signaling [30]. Collectively this suggests a relationship between TFCP2L1 and intracellular cAMP which could warrant additional investigation in future studies.

In addition to cAMP signaling, hPGCLCs in extended culture initiate DNA demethylation [27]. Using naive mouse iPSCs as a model, KLF4 and TFCP2L1 are both capable of binding ten eleven translocation 2 (TET2) at enhancers, and this is associated with targeted enhancer DNA demethylated during reprogramming [31]. TET2 is expressed in hPGCLCs, however it is unclear whether TET2, or the other TET family member regulate targeted DNA demethylation[12,32] . Future studies could address whether TFCP2L1 has a role in enhancer demethylation in hPGCLCs.

Our studies indicate that KLF4 had no role in early hPGC development, either with hPGC specification or during extended culture. In the mouse, KLF4 is reported to function redundantly with other KLF family members including KLF2 and KLF5 to regulate naive ground state pluripotency by co-binding critical pluripotent transcription factors including POU5f1, SOX2, NANOG, ESRRB[33]. Our RNA-Seq of hPGCLCs, together with previously published data sets of FACS isolated hPGCs [8,13] indicates that *KLF5 KLF11, KLF13* and *KLF16* are all highly expressed in hPGCLCs/hPGCs, whereas *KLF2* expression is below the limit of detection. Therefore, it could be hypothesized that similar to the mouse, other KLF family members substitute for KLF4 in regulating hPGC development. However, none of the KLF family members (including KLF17) were upregulated as a consequence of KLF4 knockout in hPGCLCs.

In summary, the requirement for KLF4 and TFCP2L1 in establishing naive ground state pluripotency in human pluripotent stem cells but not in hPGCLCs highlights a critical mechanistic difference in these closely related embryonic cell types, and illustrates that establishment and maintenance of pluripotency in hPGCs is critically dependent on TFAP2C. Improved late-stage modeling of hPGC development including expression of gonadal hPGC markers, together with a more detailed understanding of naive-like transcription factors in germ cell development and pluripotency, collectively provide a better understanding of causes of infertility and germ cell tumors in the context of healthy embryonic development.

Methods

Human fetal samples

All prenatal gonads were obtained from the University of Washington Birth Defects Research Laboratory (BDRL), under the regulatory oversight of the University of Washington IRB approved Human Subjects protocol combined with a Certificate of Confidentiality from the Federal Government. All consented material was donated anonymously and carried no personal identifiers, therefore the use of the de-identified fetal tissue at UCLA was deemed exempt by the UCLA IRB under 45 CRF 46.102(f). Developmental age was documented by BDRL as days post fertilization using prenatal intakes, foot length, Streeter's Stages and crown-rump length. All prenatal gonads documented with birth defect or chromosomal abnormality were excluded from this study.

Human ESC culture

The hESC lines in this study are as follows: UCLA1 (46, XX), UCLA2 (46, XY)[34], UCLA8 (46, XX)[22], and H1 OCT4-GFP (46, XY)[12]. All hESCs were cultured on mitomycin C-inactivated mouse embryonic fibroblasts (MEFs) and split every 7 days using Collagenase type IV (GIBCO, 17104-019). hESC media was comprised of 20% knockout serum replacement (KSR) (GIBCO, 10828-028), 100mM L-Glutamine (GIBCO,25030-081), 1x MEM Non-Essential Amino Acids (NEAA) (GIBCO, 11140-050), 55mM 2-Mercaptoethanol (GIBCO, 21985-023), 10ng/mL recombinant human FGF basic (Proteintech HZ1285), 1x Penicillin-Streptomycin (GIBCO, 15140-122), and 50ng/mL pri-mocin (InvivoGen, ant-pm-2) in DMEM/F12 media (GIBCO, 11330-

032). All hESC lines used in this study are registered with the National Institute of Health Human Embryonic Stem Cell Registry and are available for research use with NIH funds. hESCs used in this study were routinely tested for mycoplasma (Lonza, LT07-418). All experiments were approved by the UCLA Embryonic Stem Cell Research Oversight Committee.

Realtime PCR

Undifferentiated hESCs, iMeLCs, D4 hPGCLCs (EPCAM/ITGA6), and D4 somatic cells (the EPCAM/ITGA6 negative cells) were re-suspended in 350 uL RLT buffer (QIAGEN) and RNA was extracted using RNeasy micro kit (QIAGEN). RNA was converted to cDNA using SuperScript® II Reverse Transcriptase (Invitrogen). Real-time quantitative PCR was performed using TaqMan® Universal PCR Master Mix (Applied Biosystems), and with Taqman probes detecting expression of GAPDH, TFAP2C, SOX17, PRDM1, KLF4, and TFCP2L1. Expression levels for genes of interest were normalized to housekeeping gene GAPDH in each cell type. To quantify relative expression in each cell type, expression levels was normalized to the expression level of hESCs. hPGCLCs were compared to hESCs in biological triplicate, and to iMeLCs and somatic cells in duplicate. P-values were calculated using two-tailed student T test.

Immunofluorescence

Aggregates collected at D4, and human fetal tissue samples were fixed in 4% PFA for 1 hour, washed twice for 15 minutes in PBS, stained with hemotoxylin, and mounted in histogel (Thermo Scientific). Samples were embedded into paraffin blocks and cut onto slides in 5 um- thick sections. Slides were deparaffinized and rehydrated through a series of xlene and ethanol series. For antigen retrieval, slides were heated to 95C in Tris-EDTA solution (10 mM Tris Base, 1 mM EDTA solution, .05% Tween-20, pH9.0). Sections were permeabilized (.05% Triton-100 in PBS) for 20 minutes and blocked in PBS containing 10% normal donkey serum for 1 hour. Primary antibodies incubated overnight at 4C. Antibodies included anti-TFAP2C (sc12762; 1:100), anti-SOX17 (GT15094; 1:100), anti-Blimp1 (9115S; 1:100), anti-KLF4 (AF3640; 1:100), anti-TFCP2L1 (AF5726; 1:100), and (cKIT A405 1:100). The next day, slides were washed, blocked for an additional 30 minutes, and stained with secondary antibody for 1 hour in their corresponding species-specific secondary antibody. Secondary antibodies included donkey anti-mouse 488 IgG (715-546-150; 1:200), donkey anti-mouse 594 IgG (A21447; 1:200), donkey anti-rabbit 488 IgG (711-545-152; 1:200), donkey anti-rabbit 594 IgG (711-585-152; 1:200), donkey anti-rabbit 647 IgG (711-605-152; 1:200), donkey anti-goat 488 IgG (705-546-147; 1:200), donkey anti-goat 594 IgG KLF4, TFCP2L1 (705-586-147; 1:200), donkey anti-goat 647 IgG KLF4, TFCP2L1 (A21447; 1:200). Dapi (xxx; 1:1000) was added during secondary antibody incubation and samples were mounted in ProLong Gold antifade reagent (Invitrogen).

hPGCLCs at D4C10 or D4C21 on chamber slides, and 5iLF/A cells split onto coverslips in culture at P3 were washed and fixed in 4% PFA for 10 minutes. Cells were washed, permeabilized, blocked, and stained as described above. Primary antibodies were anti-KLF17 (042649 1:200), and anti-OCT4 (sc-5279 1:100). Secondary antibodies were incubated for 30 minutes.

For Edu analysis, cells in culture were incubated with Edu for 4 hours fixed, and detected using Click-iT™ Edu Cell Proliferation Kit for Imaging, Alexa Flour™ 488 dye before permeabilization.

Image quantification

hPGCLCs in aggregates were quantified in IMARIS 8.1 (Bitplane). For KLF4 and quantification, we counted the percentage of cells that were KLF4+ in the TFCP2C, PRDM1 double-positive hPGCLC population. This was repeated in 3 cell lines. In human fetal samples, we counted the total CKIT positive hPGCs, and then identified how many of these were KLF4 or TFCP2L1 positive. This was repeated in 6 samples for male and female each.

To identify the number of naive colonies during reversion at P3 in the mutant compared to control, 20 representative images of each sample were acquired at 10X zoom. Oct4 positive colonies were scored as full KLF17 positive, some KLF17 positive, and KLF17 negative. Counts for each category was normalized to the control.

In extended culture, total hPGCLC colonies in each well were counted and normalized to the number of cells plated down for each sample. Each was performed with 2 technical replicates. For Edu quantification, the number of Edu positive cells in each hPGCLC colony was counted and Edu percentage of each hPGCLC colony was compared between the mutant and control-dervied hPGCLCs. Error bars on graphs indicated standard error.

hESC mutants made by CRISPR/Cas9

To make null-mutations for KLF4 and TFCP2L1, pairs of gRNAs were designed to target the functionally important, most N-terminus coding region of each gene. Guides were designed using https://zlab.bio/guide-design-resources, and cloned into PX459 vector[35]. Pairs of guides were designed approximately at a 3 kB distance from each other in the genome. 4-6 days before nucleofection, UCLA1 or H1-OCT4-GFP hESCs were purified from MEFs and transferred to matrigel (BD) in mTeSR media (stemcell tech). At 70% confluence, cells were electrophorated with 4 ug of each gRNA pair was using P3 Primary Cell 4D-Nucleofector® X Kit according to the manufacturer's instructions (Lonza, V4XP-3024). 1 day following recovery, cells were dissociated with Accutase and replated on DR4 MEFs in a 6-well plate. Cells were treated with puromycin at a concentration of .35 ug/mL for 1 day. Once colonies emerge after 6-8 days, they are dissociated and plated at 10k and 50k densities in 10 cm plates. 48 colonies were picked when at the desired density afte 10 days. Colonies were split in half after 4 days. To determine homozygous mutants, we genotyped genomic DNA and chose colonies with the expected shorter band. Genotyping primers and gRNA sequences are listed in supplementary table 1. To confirm bi-allelic mutantions, mutant bands were cloned into Blunt-PCR-Cloning vector using Zero Blunt PCR Cloning Kit (TheroFisher, K270020). 5-10 colonies from each band were picked and sequenced.

hPGCLC induction

hPGCLCs were induced as described previously[22]. 1 hour before plating, 12-well plates are treated with human plasma fibronection (Invitrogen). hESCs were washed and dissociated in 0.05% trypsin for 5 minutes, and quenched with MEF media. The MEFs were removed by plating in 10-cm cell culture dishes, twice for 5 minutes each. Purified hESCs were spun, filtered with 100um filter, and seeded at a density of 200k per 12-well in iMeLC media including 15% KSR (GIBCO, 10828-028), 1x NEAA (GIBCO, 11140-050), 0.1mM 2-Mercaptoethanol (GIBCO, 21985-023), 1x Penicillin-Streptomycin-Glutamine (GIBCO, 10378-016), 1mM sodium pyruvate (GIBCO, 11360-070), 50ng/mL Activin A (Peprotech, AF-120-14E), 3mM CHIR99021 (Stemgent, 04-0004), 10mM of ROCKi (Y27632, Stemgent, 04-0012-10), and 50ng/mL primocin in Glasgow's MEM (GMEM) (GIBCO, 11710-035). After 24 hours, cells were dissociated with trypsin, inactivated with trypsin inhibitor (Sigma), resuspended in PGLCC media, and plated in ultra-low cell attachment U-bottom 96-well plates (Corning) at a density of 3k cells/well. hPGCLC media is comprised of 15% KSR (GIBCO, 10828-028), 1x NEAA (GIBCO, 11140-050), 0.1mM 2-Mercaptoethanol (GIBCO, 21985-023), 1x Penicillin-Streptomycin-Glutamine (GIBCO, 10378-016), 1mM sodium pyruvate (GIBCO, 11360-070), 10ng/mL human LIF (Millipore, LIF1005), 200ng/mL hu-man BMP4 (R&D systems, 314-BP), 50ng/mL human EGF (R&D systems, 236-EG), 10mM of ROCKi (Y27632, Stemgent, 04-0012-10), and 50ng/mL primocin in Glasgow's MEM (GMEM) (GIBCO, 11710-035).

Flow cytometry and fluorescence activated cell sorting

D4 aggregates were collected and dissociated with .05% trypsin for 10 minutes. The dissociated cells were stained with conjugated cell-surface antibodies for at least 15 minutes. Antibodies included anti-ITA6-BV421 (BioLegend, 313624 1:60), anti-EPCAM-488 (BioLegend 324210; 1:60) for UCLA-derived lines and anti-ITA6-488 (BioLegend, 313608 1:60), anti-EPCAM-APC (BioLegend 324208; 1:60) for H1-derived lines. After at least 15 minutes, cells were washed with FACS buffer (1% BSA in PBS), resuspended in FACS buffer with 7AAD (BD PharMingen 559925; 1:40). Single-cell suspensions of hESCs were used as single-color compensation controls and evaluated each with 7AAD, anti-ITA6-BC421, and anti-EPCAM-488 for UCLA1-derived lines and anti-ITA6-488, anti-EPCAM-APC, and unstained GFP-OCT4-expressing cells for the H1-OCT4-GFP derived lines. For gating controls, fluorescence-minus-one controls were made against each fluorophore, staining the residual cells from the aggregate supernatant with each antibody, minus its respective control. Gating was then established based on the absence of signal in the cell population of interest. Double-positive ITGA6, EPCAM cells were analyzed using an ARIA-H Fluorescence Activated Cell Sorter and sorted into either 350 uL of FR10 media or RLT buffer. Analysis was performed using FlowJo version 10.

For flow cytometry, cells in 5iLF/A at passage 3 were dissociated using accutase, passed through a 40um strainer (BD) and resuspended in FACS buffer at equal cell numbers. Conjugated antibodies including anti-CD75-APC (ThermoFisher 50-0759-41; 1:20), anti-CD24-BV421 (BD 562789 1:40), anti-CD90.2-APC-Cy7 (BioLegend 105327 1:20), and fixable live-dead-APC-Cy7 (Fisher 50-169-66) were diluted in staining buffer (BD 563794) and used to resuspend cell pellet, staining in the dark for at least 15 minutes. Live, non-mouse cells were gated and analyzed for their percentage of CD75 positive, CD24 negative populations. Analyses was performed on an LSR Fortessa cytometer.

Primed to Naive Reversion

Cells were reverted to the naive ground state in 5iLF/A as described previously[6,26]. At day 7, primed hESCs were dissociated into single cells with accutase and re-plated on MEFs in hESC media with Y27632 (Stemgent, 04-0012-10) at a density of 200k cells/well per 6-well plate. After one day, media was changed to 5iLAF media including a 50/50 mixture of DMEM/F12 (Gibco 11320-033) and Neurobasal (Gibco 21103-049), 1X N2 (Gibco 17502-048), 1X B27 (17504-044), 20 ng/mL rhLIF (Millipore LIF1005), 1 mM GlutaMAX (Gibco 35050-061), 1% NEAA (Gibco 11140-050), .1 mM 2-Mercaptoethanol (GIBCO, 21985-023), 1x Penicillin-Streptomycin (Gibco 15140-122), 50 ug/mL BSA (Gibco A10008-01), 1 mM PD0325901 (Stemgent 04-006-02), 1 mM IM-12 (BML-WN102-0005), .05 mM SB590885 (R&D 2650/10), 1 uM WH-4-023 (A Chemtek H620061), 10 uM Y-27632, 20 ng/mL Activin A (Peprotech AF-120-14E), 8 ng/mL FGF2 (Proteintech HZ1285), .50% KSR (Gibco 10828-028), and 1X primocin (Invitrogen (ant-pm-2). Media is changed daily and cells are passaged every 5 days at a ratio between 1:1 and 1:3 until robust colonies emerge. For quantification, 20 representative images were taken on the day of each passage 2-4. Colonies were scored as naive, primed, or intermediate. The mutant count was normalized to its corresponding control.

RNA sequencing library preparation and data analysis

Total RNA was extracted from H1-OCT4-GFP sorted D4 hPGCLCs using RNeasy micro kit (Qiagen 74004). Total RNA was reverse transcribed and cDNA was amplified using Nugen RNA-Seq System V2 (Nugen, 7102-32). DNA was extracted using MinElute PCR purification kit (Qiagen) and quantified using the Qubit dsDNA High-Sensitivity Kit (Life Technologies). Amplified cDNA was fragmented using Covaris S220 Focused-ultrasonicator. RNA-sequencing libraries were generated using Nugen Rapid Library Systems (Nugen 0320-32). Libraries were subjected to single-end 125 bp sequening on HiSeq4000 with 6 indexed libraries per lane.

RNA sequencing analysis

Raw reads in qseq format obtained from the sequencer were first converted to fastq files with a customized perl script. Read quality was evaluated with FastQC (http://www.bioinformatics.babraham.ac.uk/projects/fastqc). High-quality reads were aligned to the hg19 human reference genome using Tophat (v 2.0.13) by using “-no-coverage-search” option, allowing up to two mismatches, and only keeping unique reads. The number of unique mappable reads was quantified by HTseq (v 0.5.4) under default parameters. Expression levels were determined by RPKM (reads per kilobase of exons per million aligned reads) in R using customized scripts. For RNAseq of published datasets, GSE76970[22] and GSE93126[18], processed data of the raw read counts of each gene was utilized, with the same downstream analysis.

Extended culture

D4 hPGCLCs were cultured (C) for an additional 10 or 21 days as described previously[27]. Sorted hPGCLCs were plated at densities ranging 200-3000 cells in either a chamber well (D4C10) or 24-well (D4C21) in FR10 media. FR10 medium[36] contains 10% KSR, 2.5% FBS (Thermo Fisher Scientific, SH3007003), 1× NEAA (Gibco, 11140-050), 1 mM sodium pyruvate (Gibco, 11360070), 2 mM L-glutamine (Gibco, 25030081), 0.1 mM 2-mercaptoethanol (Gibco, 21985-023), 1× penicillin streptomycin (Gibco, 15140-122), 100 ng/mL SCF (PeproTech, 250-03), 10 μM forskolin (Sigma, F6886), 10 μM rolipram (Sigma, R6520), and 50 ng/mL primocin in Glasgow's MEM (Gibco, 11710-035). For D4C21, hPGCLCs were dissociated at D4C10 using .05% trypsin for 3 minutes. Cells are spun down at 1.6 rpm for 5 minutes, carefully resuspended, and plated at a 1:2 ratio in chamber well. Media was replaced daily until readout.

Declarations

Acknowledgements

The authors would like to thank Felicia Codrea, Jessica Scholes, and Jeffery Calimlim for FACS and Jinghua Tang for banking and culturing of the UCLA hESC lines. This work is supported by funds from an anonymous donor as well as NIH/NICHD R01 HD079546 (ATC), NIH/NIGMS P01 GM099134 (KP), and a Faculty Scholar grant from the Howard Hughes Medical Institute (KP). GH acknowledges the support of the Eli and Edythe Broad Center of Regenerative Medicine and Stem Cell Research at UCLA Training Program for supporting this work. Human fetal tissue research is supported by a grant to Ian Glass at the University of Washington Birth Defects laboratory 5R24HD000836-53. Human conceptus tissue requests can be made to bdrl@u.washington.edu.

References

1. Petropoulos, S. *et al.* Single-Cell RNA-Seq Reveals Lineage and X Chromosome Dynamics in Human Preimplantation Embryos. *Cell* **165**, 1012–1026 (2016).
2. Blakeley, P. *et al.* Defining the three cell lineages of the human blastocyst by single-cell RNA-seq. *Dev. Camb. Engl.* **142**, 3151–3165 (2015).
3. Yan, L. *et al.* Single-cell RNA-Seq profiling of human preimplantation embryos and embryonic stem cells. *Nat. Struct. Mol. Biol.* **20**, 1131–1139 (2013).
4. Hanna, J. *et al.* Human embryonic stem cells with biological and epigenetic characteristics similar to those of mouse ESCs. *Proc. Natl. Acad. Sci. U. S. A.* **107**, 9222–9227 (2010).
5. Takashima, Y. *et al.* Resetting transcription factor control circuitry toward ground-state pluripotency in human. *Cell* **158**, 1254–1269 (2014).
6. Theunissen, T. W. *et al.* Systematic identification of culture conditions for induction and maintenance of naive human pluripotency. *Cell Stem Cell* **15**, 471–487 (2014).
7. Chen, D. *et al.* The TFAP2C-Regulated OCT4 Naive Enhancer Is Involved in Human Germline Formation. *Cell Rep.* **25**, 3591-3602.e5 (2018).

8. Tang, W. W. C. *et al.* A Unique Gene Regulatory Network Resets the Human Germline Epigenome for Development. *Cell* **161**, 1453–1467 (2015).
9. Nichols, J. & Smith, A. Naive and primed pluripotent states. *Cell Stem Cell* **4**, 487–492 (2009).
10. Guo, F. *et al.* The Transcriptome and DNA Methylome Landscapes of Human Primordial Germ Cells. *Cell* **161**, 1437–1452 (2015).
11. Guo, G. *et al.* Naive Pluripotent Stem Cells Derived Directly from Isolated Cells of the Human Inner Cell Mass. *Stem Cell Rep.* **6**, 437–446 (2016).
12. Gkountela, S. *et al.* DNA Demethylation Dynamics in the Human Prenatal Germline. *Cell* **161**, 1425–1436 (2015).
13. Chen, D. *et al.* Human Primordial Germ Cells Are Specified from Lineage-Primed Progenitors. *Cell Rep.* **29**, 4568-4582.e5 (2019).
14. Kobayashi, T. *et al.* Principles of early human development and germ cell program from conserved model systems. *Nature* **546**, 416–420 (2017).
15. Sasaki, K. *et al.* The Germ Cell Fate of Cynomolgus Monkeys Is Specified in the Nascent Amnion. *Dev. Cell* **39**, 169–185 (2016).
16. Gell, J. J., Zhao, J., Chen, D., Hunt, T. J. & Clark, A. T. PRDM14 is expressed in germ cell tumors with constitutive overexpression altering human germline differentiation and proliferation. *Stem Cell Res.* **27**, 46–56 (2018).
17. Schmoll, H.-J. Extragonadal germ cell tumors. *Ann. Oncol.* **13**, 265–272 (2002).
18. Pastor, W. A. *et al.* Naive Human Pluripotent Cells Feature a Methylation Landscape Devoid of Blastocyst or Germline Memory. *Cell Stem Cell* **18**, 323–329 (2016).
19. Kojima, Y. *et al.* Evolutionarily Distinctive Transcriptional and Signaling Programs Drive Human Germ Cell Lineage Specification from Pluripotent Stem Cells. *Cell Stem Cell* **21**, 517-532.e5 (2017).
20. Ye, S., Li, P., Tong, C. & Ying, Q.-L. Embryonic stem cell self-renewal pathways converge on the transcription factor Tfcp2l1. *EMBO J.* **32**, 2548–2560 (2013).
21. Pontis, J. *et al.* Hominoid-Specific Transposable Elements and KZFPs Facilitate Human Embryonic Genome Activation and Control Transcription in Naive Human ESCs. *Cell Stem Cell* **24**, 724-735.e5 (2019).
22. Chen, D. *et al.* Germline competency of human embryonic stem cells depends on eomesodermin. *Biol. Reprod.* **97**, 850–861 (2017).
23. Sasaki, K. *et al.* Robust In Vitro Induction of Human Germ Cell Fate from Pluripotent Stem Cells. *Cell Stem Cell* **17**, 178–194 (2015).
24. Li, L. *et al.* Single-Cell RNA-Seq Analysis Maps Development of Human Germline Cells and Gonadal Niche Interactions. *Cell Stem Cell* **20**, 858-873.e4 (2017).
25. Liu, X. *et al.* Comprehensive characterization of distinct states of human naive pluripotency generated by reprogramming. *Nat. Methods* **14**, 1055–1062 (2017).

26. Collier, A. J. *et al.* Comprehensive Cell Surface Protein Profiling Identifies Specific Markers of Human Naive and Primed Pluripotent States. *Cell Stem Cell* **20**, 874-890.e7 (2017).
27. Gell, J. J. *et al.* An Extended Culture System that Supports Human Primordial Germ Cell-like Cell Survival and Initiation of DNA Methylation Erasure. *Stem Cell Rep.* (2020) doi:10.1016/j.stemcr.2020.01.009.
28. Wang, X. *et al.* The transcription factor TFCP2L1 induces expression of distinct target genes and promotes self-renewal of mouse and human embryonic stem cells. *J. Biol. Chem.* **294**, 6007–6016 (2019).
29. Wang, Z. *et al.* Meta-analysis of five genome-wide association studies identifies multiple new loci associated with testicular germ cell tumor. *Nat. Genet.* **49**, 1141–1147 (2017).
30. Henderson, Y. C., Frederick, M. J., Wang, M. T., Hollier, L. M. & Clayman, G. L. LBP-1b, LBP-9, and LBP-32/MGR Detected in Syncytiotrophoblasts from First-Trimester Human Placental Tissue and Their Transcriptional Regulation. *DNA Cell Biol.* **27**, 71–79 (2008).
31. Sardina, J. L. *et al.* Transcription Factors Drive Tet2-Mediated Enhancer Demethylation to Reprogram Cell Fate. *Cell Stem Cell* **23**, 727-741.e9 (2018).
32. Vincent, J. J. *et al.* Stage-specific roles for tet1 and tet2 in DNA demethylation in primordial germ cells. *Cell Stem Cell* **12**, 470–478 (2013).
33. Jiang, J. *et al.* A core Klf circuitry regulates self-renewal of embryonic stem cells. *Nat. Cell Biol.* **10**, 353–360 (2008).
34. Diaz Perez, S. V. *et al.* Derivation of new human embryonic stem cell lines reveals rapid epigenetic progression in vitro that can be prevented by chemical modification of chromatin. *Hum. Mol. Genet.* **21**, 751–764 (2012).
35. Ran, F. A. *et al.* Genome engineering using the CRISPR-Cas9 system. *Nat. Protoc.* **8**, 2281–2308 (2013).
36. Ohta, H. *et al.* In vitro expansion of mouse primordial germ cell-like cells recapitulates an epigenetic blank slate. *EMBO J.* **36**, 1888–1907 (2017).

Figures

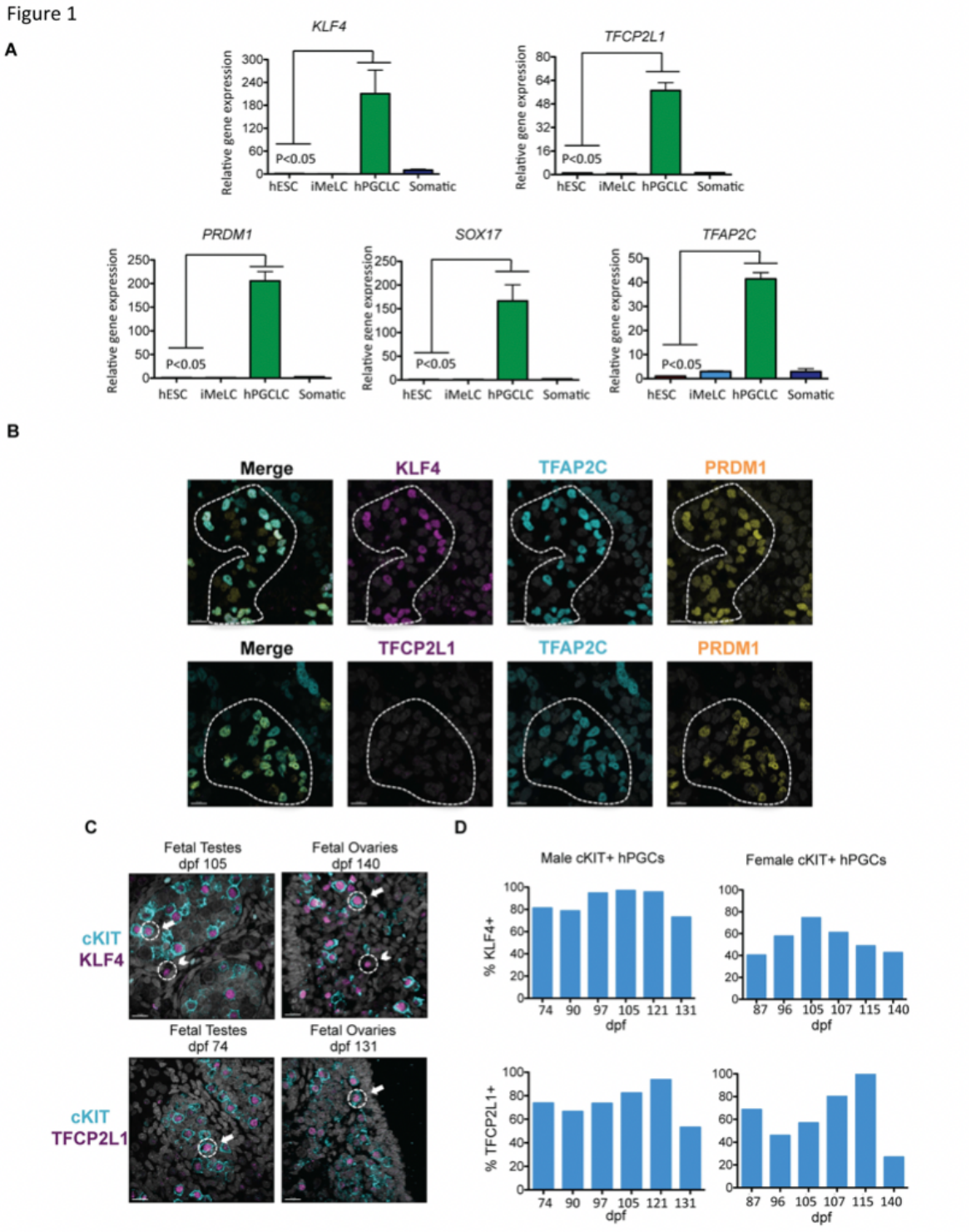

Figure 1

KLF4 and TFCP2L1 RNA and protein expression during hPGC development. a. Quantitative real-time rt-PCR of KLF4 and TFCP2L1 in hESCs, iMeLCs, and hPGCLCS plus somatic aggregate cells from the UCLA1 hESC line at day 4 (D4) of differentiation. n=3 independent replicates of hESC and hPGCLCs. T-test was used to determine significance between these two groups. b. Representative immunofluorescence for KLF4 and TFCP2L1 in TFAP2C/PRDM1 double positive hPGCLCs at D4 (n= 8

aggregates of UCLA8). c. Representative immunofluorescence images of embryonic and fetal ovaries and testes at indicated days post fertilization (dpf): Arrows highlight double positive hPGCs, Arrow head indicates single positive somatic cells. d. Quantification of the percentage KLF4 or TFCP2L1 positive cKIT+ hPGCs at each time point. (n= 89-530 cKIT+ hPGCLCs counted per time point). Scale bars show 15 microns.

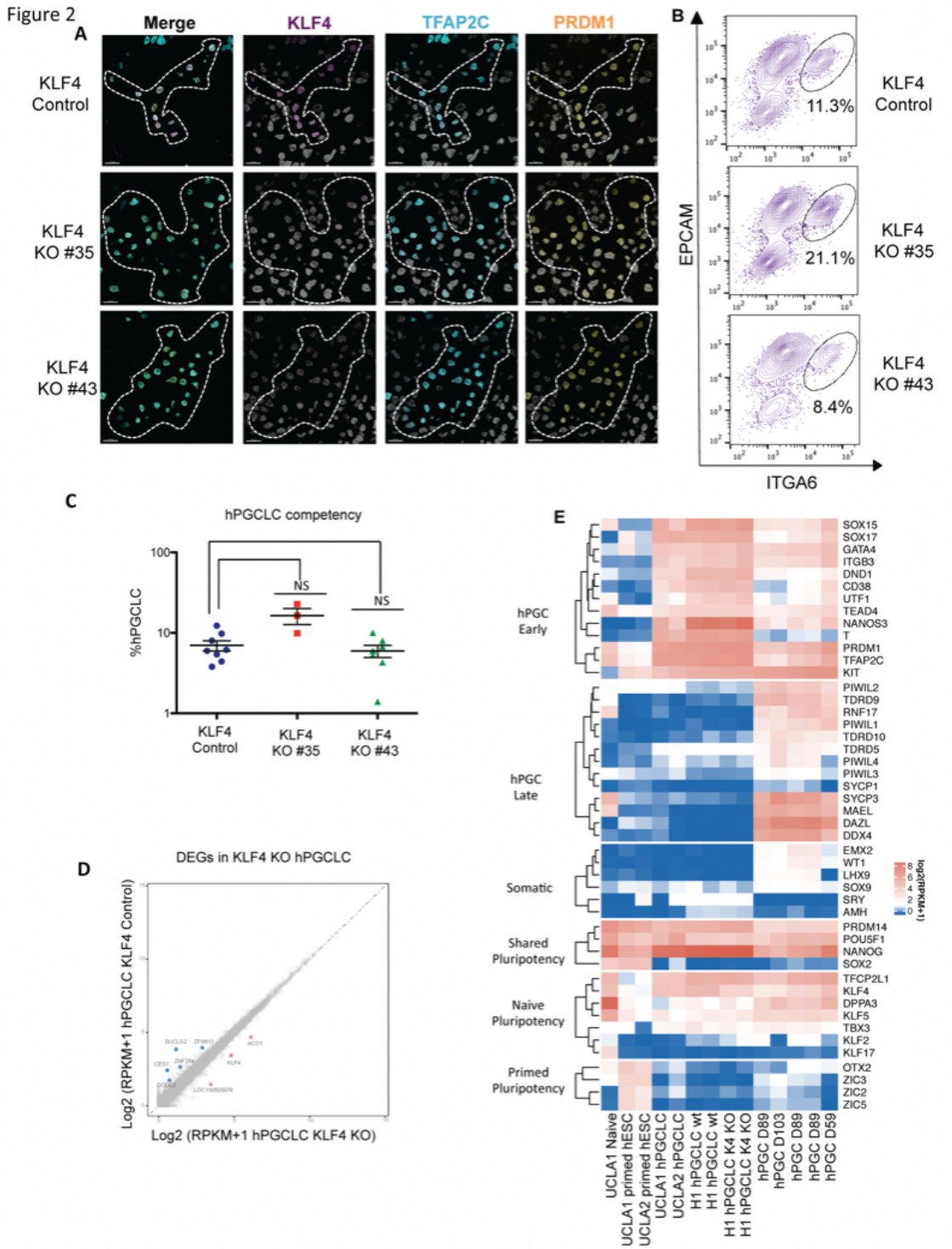

Figure 2

KLF4 knockdown does not affect hPGC specification. a. Representative image of TFAP2C/PRDM1 co-expressing hPGCLCs in KLF4 control and mutant aggregates at D4 using the UCLA1 hESC sublines (n= 5 aggregates). b. Representative FACS plots showing EPCAM/ITGA6 double-positive hPGCLCs in control and mutant aggregates at D4. c. Quantification of the percentage ITGA6/EPCAM hPGCLCs in control (n= 8 biological replicates) and KLF4 mutant sublines (n=3 and n=7 biological replicates respectively). d. RNA-Seq gene expression normalized between KLF4 mutant and control lines highlighting differentially upregulated genes (n=2 independent replicates) e. Heatmap of diagnostic gene expression comparing KLF4 KO and control sublines to wildtype hPGCs, hPGCLCs, naive and primed cells. Scale bars = 15 microns.

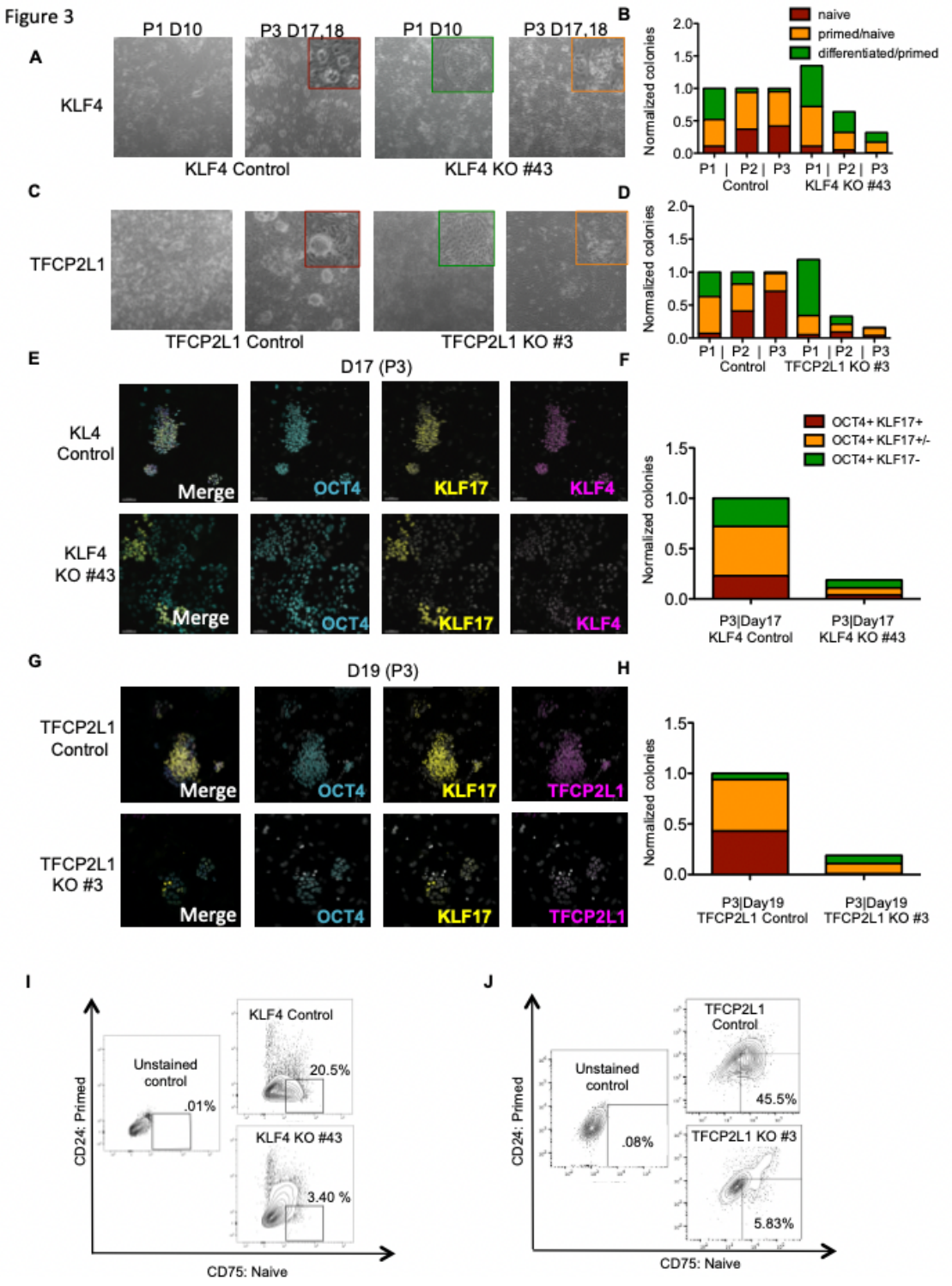

Figure 3

KLF4 and TFCP2L1 are required for reversion to the naive ground state. a. Representative bright field images of KLF4 control (left) and KO (right) sublines during reversion at D10 and D17. Insert shows naive colony (red), partial primed/naive colony (yellow), and differentiated/primed colony (green). b. Quantification of colony scoring across all images during reversion (n= 176-734 colonies evaluated for each time point). c. Representative bright field images for TFCP2L1 control and KO evaluated as in (a). d.

Quantification for TFCP2L1 reversion as in (b) (n= 22-138 colonies evaluated for each time point). e. Representative immunofluorescence image of D17 reversions with KLF4 control and KO sublines f. Quantification of colony type by KLF17 expression with OCT4 (n=631 and 111 colonies analyzed for control and mutant). g. Representative immunofluorescence image of D19 reversions with TFCP2L1 control and mutant sublines. h. Quantification of colony type by KLF17 expression with OCT4 (n= 83 and n=16 colonies analyzed for control and mutant). i. Flow cytometry analysis for CD75-positive, CD24-negative naive populations at D17 of reversion in KLF4 control and KO. Gating set by unstained controls. j. Same as i with TFCP2L1 control and KO sublines at D18.

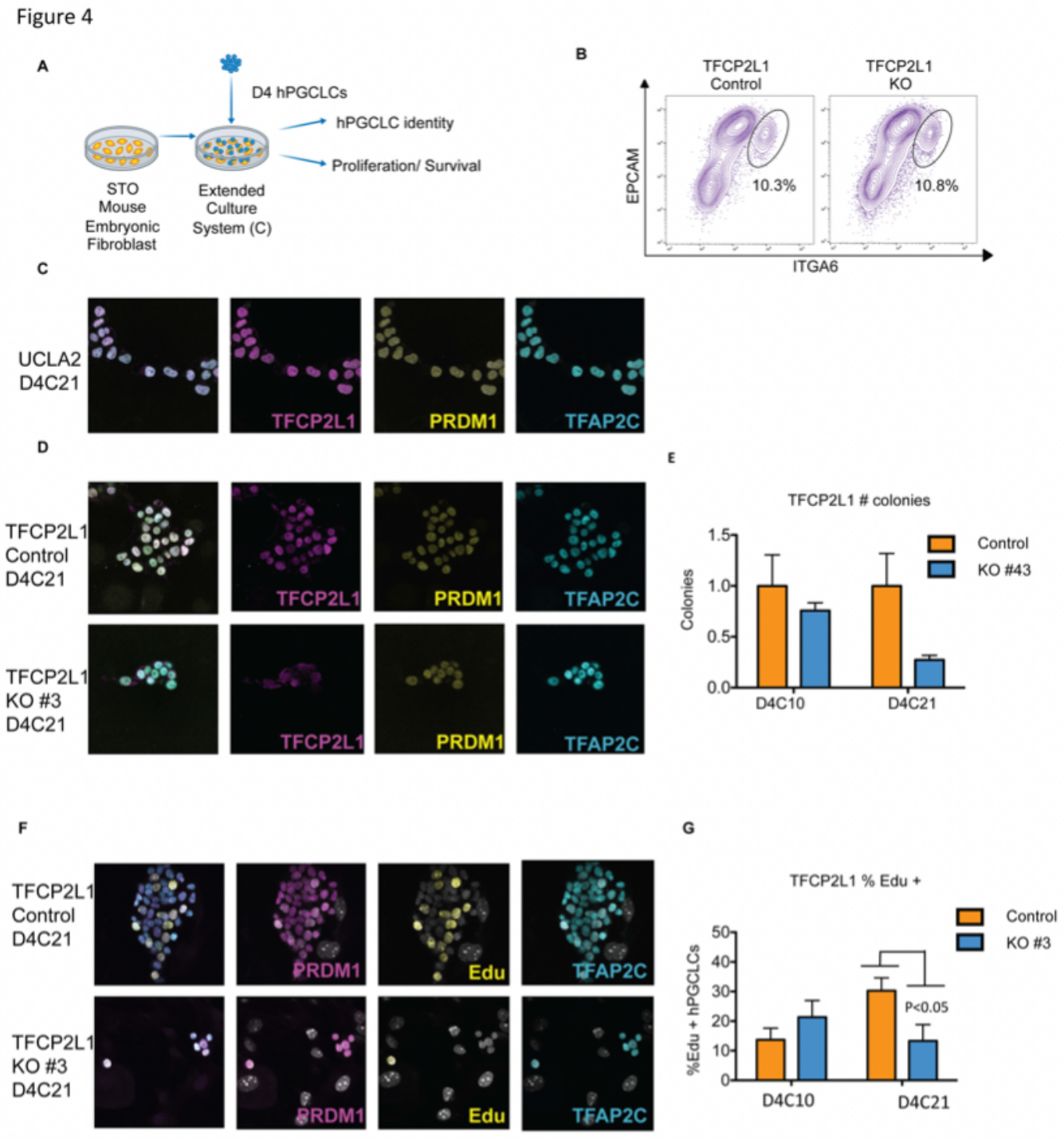

Figure 4

TFCP2L1 in extended hPGCLC culture. a. Schematic of D4 hPGCLCs grown in extended culture (C). Analysis of extended culture is referred to as D4CX. b Representative FACS plots for ITGA6, EPCAM double-positive hPGCLCs in TFCP2L1 control and mutant sublines. c. Representative immunofluorescence image of wildtype UCLA2 hPGCLCs at D4C21 (n= 10 colonies analyzed) d. Representative immunofluorescence image of TFCP2L1 control and KO hPGCLCs at D4C21. e.

Quantification of the number of hPGCLC colonies in each experimental condition (n= 5 to 75 different colonies counted). f. Representative immunofluorescence image of TFCP2L1 control and KO hPGCLCs with Edu staining. g. Quantification of percentage of Edu+ cells within a hPGCLC colony. Error bars indicate n=4-10 colonies analyzed. Scale bars = 10 microns

Supplementary Files

This is a list of supplementary files associated with this preprint. Click to download.

- Supplement20200407Hancock.docx